Supporting Information

Binding Interface and Electron Transfer Between Nicotine Oxidoreductase and its Cytochrome c Electron Acceptor

*Elizabeth J. Mumby, Jamin A. Willoughby Jr., Cristian Vasquez, Niusha Delavari, Zhiyao Zhang, Christopher T. Clark, and Frederick Stull**

Department of Chemistry, Western Michigan University, Kalamazoo, Michigan 49008, United States

*Corresponding author. Email: frederick.stull@wmich.edu

Experimental Procedures

Modeling of the NicA2-CycN complex using AlphaFold2 Multimer

The structure of the NicA2 homodimer-CycN complex was prepared using the AlphaFold2 Multimer (1.0) complex prediction extension of AlphaFold2[1] in the COSMIC2 gateway[2]. The mature sequence for NicA2 (Uniprot Accession F8G0P2) and CycN (Uniprot Accession A0A0E3ELC2) from *Pseudomonas putida* S16 after removing the signal peptides (residues 39-482 for NicA2 and residues 28-132 for CycN) were used for complex prediction. The input used for AlphaFold2 Multimer included two copies of the NicA2 sequence (to account for the NicA2 homodimer) and one copy of the CycN sequence. The output from the COSMIC2 gateway included five models whose per residue local distance difference test confidence score (pLDDT) ranged from 0.92-0.95. All five models had CycN positioned in the same location on NicA2's surface, with small differences in the orientation of surface exposed side chains in the five models. The model with the highest pLDDT is the one used throughout this paper. AlphaFold Multimer does not include cofactors in its structural predictions; thus, the position of the FAD for NicA2 and the heme for CycN in the model was obtained by aligning the structure of the NicA2 dimer (PDB 6C71)[3] and CycN (PDB 7TLX)[4] on the model generated by AlphaFold Multimer.

Cloning and mutagenesis

The synthesized codon-optimized *nicA2* gene obtained previously[5] was cloned into the NdeI and XhoI sites of pET22b vector using Gibson Assembly while keeping the restriction sites strictly intact. The resulting pET22b based construct results in a C-terminally His tagged version of NicA2 that allows for purification of pBpa-containing proteins. Site-directed mutagenesis was used to individually replace codons for the following amino acid residues with the amber codon (TAG) in this NicA2 construct: Arg78, Ser86, Phe93, Arg96, Phe104, Asp136, Ser146, Glu154,

Glu172, Arg187, Lys199, Arg205, Gln255, Thr267, Met275, Asn286, Lys290, Asp295, Lys324, Lys331, Lys346, Tyr370, Glu386, Arg393, Pro405, Phe422, Lys439 and Arg447. A pEVOL plasmid which expresses an aminoacyl-tRNA synthetase/tRNA pair was co-transformed into BL21 (DE3) *Escherichia coli* with each NicA2 mutant construct and plated on LB containing 100 μg/mL ampicillin and 34 μg/mL chloramphenicol. The aminoacyl-tRNA synthetase/tRNA pair allows the incorporation of p-benzoyl-L-phenylalanine (pBpa) into each NicA2 mutant.[6] Mutagenesis to replace Trp108, Tyr415, Trp417 and Trp427 with Phe was done in the original N-terminal His-SUMO tagged pET28a based construct.[5]

Expression and purification

Expression of the pBpa-containing variants was done in 1 L cultures of protein expression media (24 g/L yeast extract, 12 g/L tryptone, and 4% v/v glycerol which was then supplemented with an additional 10% v/v phosphate buffer containing 0.17 M KH_2PO_4 and 0.72 M K_2HPO_4 after autoclaving) containing 100 μg/mL ampicillin, 34 μg/mL chloramphenicol. The pBpa was dissolved in 1 M NaOH before it was added to the media at a final concentration of 1 mM. Omission of pBpa from the cultures resulted in no production of any of the NicA2 variants containing the amber codon. Cultures were grown at 37°C with oscillation until an A_{600} of 1.0. The temperature was then lowered to 20°C and expression of each NicA2 variant was induced with 100 μM IPTG and expression of the pBpa aminoacyl-tRNA synthetase tRNA pair was induced with 0.2% w/v L-arabinose. Cultures were left to grow overnight at 20°C. Cells collected by centrifugation were then lysed at 4°C via sonication in buffer containing: 50 mM $NaPO_4$, 300 mM NaCl, 20 mM imidazole, and 10% glycerol v/v at pH 8 (lysis buffer) with benzonase nuclease and protease cocktail inhibitor. Cell debris was removed from lysate via centrifugation and lysate loaded onto gravity columns containing Ni-NTA resin. The columns were washed with five

column volumes of lysis buffer and NicA2 was eluted into buffer composed of: 50 mM $NaPO_4$, 300 mM NaCl, 250 mM imidazole, and 10% glycerol v/v at pH 8. Protein was buffer exchanged into 40 mM HEPES-KOH pH 7.5, 100 mM NaCl, 10% glycerol and stored at 4°C until use. Expression and purification of CycN and Trp108Phe, Tyr415Phe, Trp417Phe and Trp427Phe NicA2 mutants in the N-terminal His-SUMO construct were purified as described previously.[4,5]

Attempted in vitro crosslinking

Mixtures containing 10-50 μM NicA2 variant and 5-50 μM CycN in 40 mM HEPES-KOH pH 7.5, 100 mM NaCl, 10% glycerol or PBS were exposed to either a handheld UVP 365 nm lamp or a Eurosolar facial tanning lamp[7] for 10 min to 24 hr on ice in 1.5 mL microcentrifuge tubes, PCR tubes or 96 well plates. The samples were then run on a 4-12% Bis-Tris SDS-Page gel and the gel was stained with TMBZ (heme stain) to identify the presence of CycN.[8] This was done by first dissolving 6.3 mM of 3, 3', 5, 5'-tetramethylbenzidine (TMBZ) into 30 mL of methanol. After dissolving, 70 mL of 0.25 M sodium acetate was added to the solution. The gels were rinsed in water and then submerged in this solution. While in solution, the gels were incubated at room temperature, oscillated occasionally, and placed in the dark for two hours. 495 μL of 30% v/v hydrogen peroxide was then added to the gel bath. Gels were then incubated for an additional 30 minutes at room temperature in the dark with vigorous oscillation to develop the stain. The staining solution was then removed, yielding dark blue bands where CycN was located. Only bands at ~12 kDa were detected, consistent with free CycN. Some representative images of this are shown in **Figure S1**.

Activity assays

In a 96-well plate, 20 μM CycN, 1 nM NicA2 mutant, and 1 mM nicotine were combined in PBS in a 100 μL total reaction volume and the change in absorbance of the reaction at 550 nm

over time was measured at room temperature using a TECAN M-1000 plate reader. Nicotine was added as the last component of the reaction and directly before beginning absorbance readings. Reactions were performed in triplicate with each mutant. A reaction containing only CycN and nicotine was also performed in triplicate to measure the spontaneous background reaction rate between CycN and nicotine. Reaction rates measuring absorbance were converted to concentration based on the 21,000 $M^{-1}cm^{-1}$ change in extinction coefficient at 550 nm upon CycN reduction and divided by two to account for the use of two CycN molecules for each catalytic cycle.[5,9]

Stopped-flow experiments

All stopped-flow experiments were preformed anaerobically in buffer containing: 40 mM HEPES, 100 mM NaCl, and 10% v/v glycerol adjusted to pH 7.5 with KOH at 4°C using a TgK Scientific SF-61DX2 KinetAsyst instrument with Kinetic Studio software. All experiments measuring the reaction between NicA2 mutant and nicotine were conducted using 25 μM of NicA2 mutant (FAD concentration) before mixing. For all experiments measuring the reaction between NicA2 mutants and CycN, 30 μM of NicA2 (FAD concentration) was utilized. For every experiment, solutions of NicA2 mutant and CycN were created in anaerobic tonometers where oxygen was removed by cycling the tonometer through exposures of vacuum and anaerobic argon.[10] For experiments with CycN and the pBpa-containing mutants, NicA2 solutions were anaerobically titrated with a 2 mM nicotine solution to reduce the flavin. This nicotine solution was made anaerobic and placed in a gas-tight Hamilton syringe. Nicotine was added until NicA2's flavin reached a fully reduced state. Absorbance of NicA2's flavin was monitored using a Cary 50 Bio UV-Visible Spectrophotometer and Cary WinUV software. For experiments monitoring the reaction between CycN and Trp108Phe, Tyr415Phe, Trp417Phe, Trp427Phe or Tyr415Phe/Trp417Phe NicA2, NicA2's flavin was reduced using dithionite. Dithionite was used

as a reductant for these experiments to eliminate any possible effect on the kinetics caused by a decrease in binding affinity for N-methylmyosmine in the phenylalanine-containing mutants since these residues form part of the substrate binding site and we have previously observed that N-methylmyosmine binding decreases the rate constants for electron transfer to CycN in the oxidative half-reaction by 3-7 fold.[5] However, dithionite reacts quite slowly with NicA2's FAD, making it less convenient to use as a reductant for oxidative half-reaction experiments than nicotine, which reacts quickly with NicA2's FAD. Accordingly, nicotine was used as the reductant for oxidative half-reaction experiments with the pBpa-containing variants since these substitutions are on the surface of NicA2 far from the substrate binding site and are therefore less likely to affect the affinity for N-methylmyosmine.

For the NicA2 mutant reactions with nicotine, the anaerobic oxidized NicA2 was loaded onto the stopped-flow and then mixed with 200 μM of nicotine before mixing (made anaerobic by sparging with argon). For the reactions measuring the reaction between NicA2 and CycN, the reduced NicA2 solution was loaded onto the instrument and mixed with 80 μM CycN (before mixing). Absorbance changes for the NicA2 reactions with nicotine were monitored using the instrument's single-wavelength detector at 450 nm with the photomultiplier tube. Reactions between the NicA2 mutants and CycN were measured using the instrument's multi-wavelength charge-coupled device detector. Kinetic traces were exported to KaleidaGraph where they were fitted to Equation 1 (reactions with CycN) or Equation 2 (reactions with nicotine) as described previously[5] to obtain k_{obs} values.

$$Y = \Delta A_1 e^{-k_{obs1}t} + \Delta A_2 e^{-k_{obs2}t} + A_\infty \quad (1)$$

$$Y = \Delta A_1 e^{-k_{obs1}t} + \Delta A_2 e^{-k_{obs2}t} + \Delta A_3 e^{-k_{obs3}t} + A_\infty \quad (2)$$

In Equations 1 and 2, ΔA is the kinetic amplitude for each phase, k_{obs} is the apparent first order rate constant and A_∞ is the absorbance at the end of the reaction.

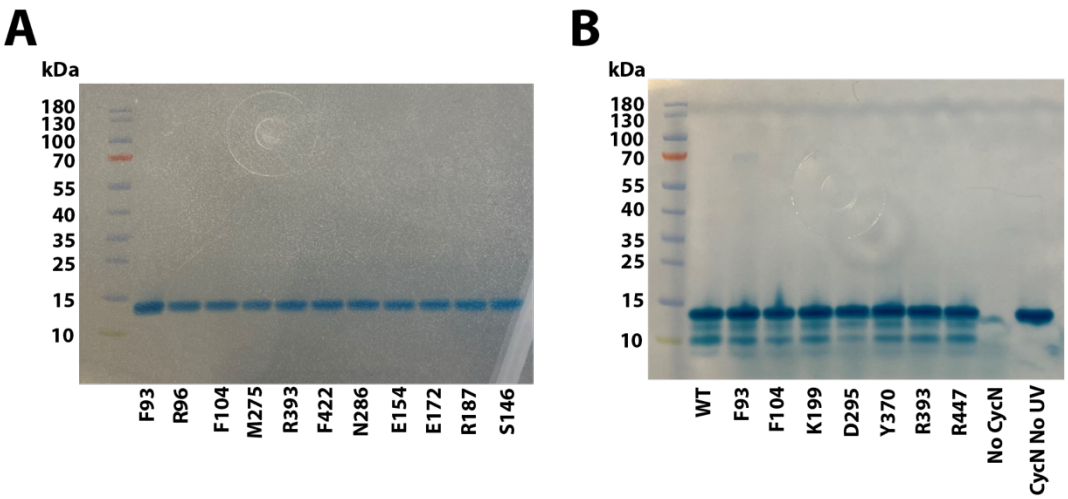

Figure S1. Attempted crosslinking and heme staining. Note that the heme of CycN is covalently attached to the protein. (A) Heme staining of 5 μM CycN with 10 μM pBpa-containing NicA2 variant exposed to hand-held 365 nm UV lamp for 1 hour. (B) Heme staining of 50 μM CycN with 50 μM pBpa-containing NicA2 variant exposed to a Eurosolar UV lamp for 30 minutes. The faint band at ~70 kDa for the sample containing pBpa at position Phe93 was not reproducible.

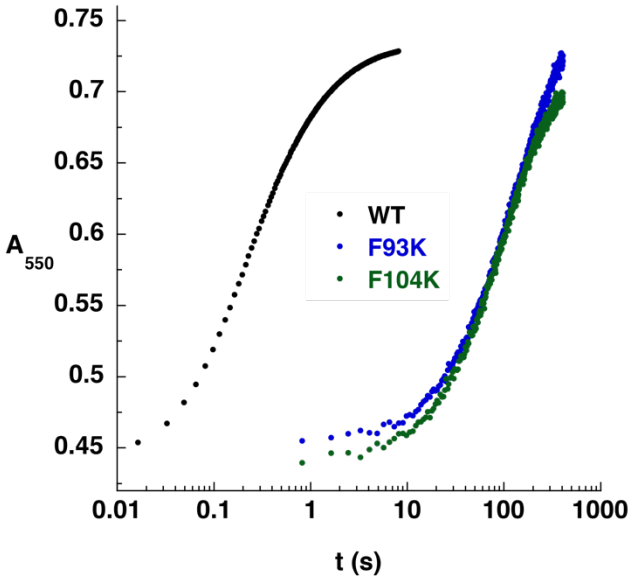

Figure S2. Stopped-flow absorbance traces for the oxidative half-reaction of NicA2 mutant enzymes with CycN. Note the logarithmic time base. Traces for Phe93Lys and Phe104Lys NicA2 fit best to a single exponential function, yielding k_{obs} values of 0.0074 s^{-1} and 0.0095 s^{-1}, respectively.

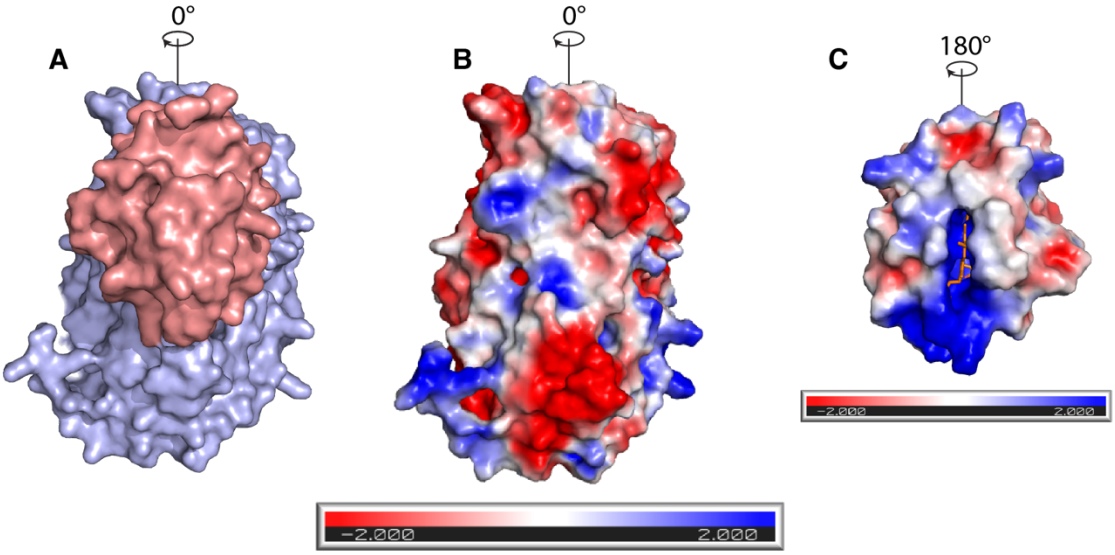

Figure S3. (A) Structure of the NicA2-CycN complex predicted by AlphaFold Multimer. NicA2 is shown in light blue and CycN is shown in salmon. Only one protomer of the NicA2 dimer is shown for clarity. (B) and (C) Surface charge distribution of NicA2 and CycN, respectively, calculated using the APBS electrostatics plugin of PyMOL.[11] The structure of CycN has been rotated 180 degrees relative to that shown in panel A in order to display the surface that interacts with NicA2. Red color indicates negative charge density; blue color indicates positive charge density; the heme cofactor is colored in orange in panel C.

```
NicA2       --MSDKTKTNEGFSRRSFIGSAAVVTAG--VAG-LGAIDAASATQKTNRASTVKGGFDYD      55
Pnad        MTKDGDEGSKSGVSRRKFLGSAAVGVATAGIASQLLTLSAPAEAAVKTNVGPSRAGVGYD      60
NdpB        ----------------------------------------------------MTEKIYD      7
6HLNO       ----------------------------------------------------METSD      5
MAO_N       ------MTSRDGYQWTP-----ETG-LTQGVP-SLGVISPPTNIE------DTDKDGPWD      41
MAO_A       ---------------------------------------MENQEKASIAGHMFD          15

NicA2       VVVVGGGFAGATAARECGLQGYRTLLLEARSRLGGRTFTSRFAG-QEIEFGGAWVHWLQP      114
Pnad        VIVIGGGFAGVTAAREASRSGLKTLILEGRSRLGGRTFTSKLQN-QKVELGGTWVHWTQP      119
NdpB        AIVVGAGFSGLVAARELSAQGRSVLIIEARHRLGGRTHVVNFLG-RPVEIGGAGVHWCQP      66
6HLNO       VIVIGAGFAGLTAARELSRSGHATIVLEAKDRIAGRTHLAERLG-RNLELGGTWVHWTQP      64
MAO_N       VIVIGGGYCGLTATRDLTVAGFKTLLLEARDRIGGRSWSSNIDG-YPYEMGGTWVHWHQS      100
MAO_A       VVVIGGGISGLSAAKLLTEYDVSVLVLEARDRVGGRTYTIRNEHVDYVDVGGAYVGPTQN      75

NicA2       HVWAEMQRYGLGVVEDPLTNLDKTLIMYNDGSV----ESISPDEFGKNIRIAFEKLC---      167
Pnad        NVWTEIMHYGLEVEETVGLANPETVIWVTEDNV----KRAPAAEAFEIFGSACNEYY---      172
NdpB        HVFAEMQRYGFGFKEAPLADLDKAYMVFADGQK----IDVPPATFDEEYTTAFEKFC---      119
6HLNO       YVWAEMGRYGIKALPGPEF--T-KALWTLGGQR----HEGSPERLMELLDGPNRLLL---      114
MAO_N       HVWREITRYKMHNALSPSFNFSRGVNHFQLRTNPTTSTYMTHEAEDELLRSALHKFTNVD      160
MAO_A       RILRLSKELGIETYK---VNVSERLVQYVKGKTYPFRGAFPPVWNPIAYLDYNNLWRTID      132

NicA2       -HDAWEVFPRPHEPMFTE-RARELDKSSVLDRIKTLG--LSRLQQAQINSYMALYAGETT      223
Pnad        -KEARNIYPRPFEPFFERKKLQHVDGLSAADYLEKLP--LTREQKDMMDSWLSGNGHNYP      229
NdpB        -SRSRELFPRPYSPLDNH-EVSNLDGVSARDHLESLG--LNELQLASMNAELTLYGGAPT      175
6HLNO       -ADSRRYFPMPWQPLDNP-DVADIDGITLSEAIDRLG--LPEDQRRLLRSFWTLNFNGRL      170
MAO_N       GTNGRTVLPFPHDMFYVP-EFRKYDEMSYSERIDQIRDELSLNERSSLEAFILLCSGGTL      219
MAO_A       NM-GK---EIPTDAPWEAQHADKWDEMTMKELIDKIC--WTKTARRFAYLFVNINVTSEP      186

NicA2       DKFGLPGVLKLFACGGWNYD--AFMDTETHYRIQGGTIGLINAMLTDS----GAEVRMSV      277
Pnad        ETIAYSEIMRWFALSNFNMP--TMFDSIARYKIKTGTHSLLEAIMADG----NSEVKLST      283
NdpB        TELSYPSFVKFHALASWDTI--TFTDSEKRYHVQGGTNALCQAIFDDC----RADSEFGV      229
6HLNO       DEAAYTQALRWCAVASGDWQ--LMFEACASFKIDGGTRRLAEAILADS----SAQLRLKQ      224
MAO_N       ENSSFGEFLHWWAMSGYTYQ--GCMDCLISYKFKDGQSAFARRFWEEAAGTGRLGYVFGC      277
MAO_A       HEVSALWFLWYVKQCGGTTRIFSVTNGGQERKFVGGSGQVSERIMDLL----GDQVKLNH      242

NicA2       PVTAVEQVNGGVKIKTDDDEIITAGVVVMTVPLNTYKHIGFTPALSKGKQRFIKEGQLSK      337
Pnad        PVTKVNQDKDKVTVTTED-GVFTASAVIVAVPINTLHDIEYSPKLSAAKVDMGSQRHAGA      342
NdpB        PVEAVAQTDNGVTVTLADKRVFRALTCVLTLPTKVYADVRFEPPLPPEKRAFIEHAEMAD      289
6HLNO       RVVSVEQDAGGVLVATEAGEQYRARQVILALPLSVLNGIDVHPPLSPGKREAAARGQAGR      284
MAO_N       PVRSVVNERDAARVTARDGREFAAKRLVCTIPLNVLSTIQFSPALSTERISAMQAGHVNM      337
MAO_A       PVTHVDQSSDNIIIETLNHEHYECKYVINAIPPTLTAKIHFRPELPAERNQLIQRLPMGA      302

NicA2       GAKLYVHVKQNLGRVFAFAD------EQQPLNWVQT---HDYSDELGTILSITIARKET-      387
Pnad        GVKGYIRVKQNVGNVMTYAP------ARNKLTPFTSVF-TDHVDESGTLLIAFSADPKL-      394
NdpB        GAELYVHVRQNLGNTFTFCD------DPNPFNAVQT---YAYDDELGTILKITIGRQSL-      339
6HLNO       GAKLWIKVDGRQERFVAFGP------ETAALNFVQA----EYIDQDTTTLVCFGPDAGA-      333
MAO_N       CTKVHAEVDNKDMRS--WTG------IAYPFNKLCYAIGDGTTPAGNTHLVCFGTDANH-      388
MAO_A       VIKCMMYYKEAFWKKKDYCGCMIIEDEDAPISITLD---DTKPDGSLPAIMGFILARKAD      359

NicA2       --IDVN----------DRDAVTREVQKMFPGV-EVLGTAAYDWTADPFSLGAWAAYG-VG      433
Pnad        --IDIN----------DIKAVEKALQPLLPGV-EVTASYGYDWNLDPFSKGTWCTYR-PN      440
NdpB        --INLE----------NFDAIAAEIRKIHGDV-EVLEALPYNWAMDEYARTSYPAMR-KG      385
6HLNO       --VDVD----------DVAEAQGHLDAIVPGL-KVLEVAGHDWVSDEYARSTWPMHY-TG      379
MAO_N       --IQPD---------EDVRETLKAVGQLAPGTFGVKRLVFHNWVKDEFAKGAWFFSR-PG      436
MAO_A       RLAKLHKEIRKKKICELYAKVLGSQEALHPV-----HYEEKNWCEEQYSGGCYTAYFPPG      414

NicA2       QLSRL-KDLQAAEGRILFAGAETSNGWHANIDGAVESGLRAGREVKQLLS----------      482
Pnad        QTTRYLTELQKREGRLFFAGSDMANGWRGFIDGAIENGREVGHQVATYLKRENDNA----      496
NdpB        WFSRY-KDMAKPENRLFFAGSATADGWHEYIDGAIESGIRVGREIRHFMKATA-------      437
6HLNO       YLTRHLAELQRPEGRIRLAGSDFANGWGGFIDGAIESGFDAARQVASALTSDTRPPLRAP      439
MAO_N       MVSECLQGLREKHRGVVFANSDWALGWRSFIDGAIEEGTRAARVVLEELGTKREVKARL-      495
MAO_A       IMTQYGRVIRQPVGRIFFAGTETATKWSGYMEGAVEAGERAAREVLNGLGKVTEKDIWVQ      474
```

```
NicA2       ----------------------------------------------------    482
Pnad        ----------------------------------------------------    496
NdpB        ----------------------------------------------------    437
6HLNO       APVG------------------------------------------------    443
MAO_N       ----------------------------------------------------    495
MAO_A       EPESKDVPAVEITHTFWERNLPSVSGLLKIIGFSTSVTALGFVLYKYKLLPRS    527
```

Figure S4. Full-length alignment of NicA2 and Pnad from *Pseudomonas putida* S16 and closely related flavoprotein amine oxidase homologs that have been biochemically established as oxidases. Residues on the surface of NicA2 at the CycN binding site identified in this study are highlighted in yellow. Red stars indicate locations where replacement with pBpa in NicA2 results in a substantial decrease in rate constants for electron transfer to CycN (**Figure 2D** of main text). NdpB, L-hydroxynicotine oxidase from *Shinella* sp. HZN7[12,13]; 6HLNO, L-hydroxynicotine oxidase from *Arthrobacter nicotinovorans*[14,15]; MAO_N, Monoamine oxidase-N from *Aspergillus niger*[16,17]; MAO_A, Monoamine oxidase A from *Homo sapiens*[18,19].

Table S1. Observed rate constants for the reductive half-reaction of pBpa containing NicA2 variants[a,b]

NicA2 variant	k_{obs1} (s^{-1})	k_{obs2} (s^{-1})	k_{obs3} (s^{-1})
WT	178	36.7	1.3
Phe93	230	74.1	0.75
Phe104	221	61.4	1.81
Lys199	169	46.5	2.32
Asp295	171	78.3	2.73
Tyr370	49.9	14.4	0.37
Arg393	268	94.2	0.95
Arg447	168	52.1	2.54

[a]Obtained by fitting traces in **Figure 3A** to Equation 2
[b]See **Scheme S1** for kinetic scheme and steps represented by rate constants.

Table S2. Observed rate constants for the oxidative half-reaction of pBpa containing NicA2 variants[a,b,c]

NicA2 variant	k_{obs1} (s^{-1})	k_{obs2} (s^{-1})
WT	4.85	0.79
Phe93	0.0038[d]	
Phe104	0.092	0.021
Lys199	5.62	0.83
Asp295	0.22	0.02
Tyr370	5.41	0.79
Arg393	1.18	0.28
Arg447	5.89	1.07

[a]Obtained by fitting traces in **Figure 3B** to Equation 1
[b]NicA2's FAD was reduced with one equivalent of nicotine (see Experimental Procedures)
[c]See **Scheme S2** for kinetic scheme and steps represented by rate constants.
[d]Estimate from fitting to a single exponential function

Table S3. Observed rate constants for the oxidative half-reaction of phenylalanine containing NicA2 variants[a,b,c]

NicA2 variant	k_{obs1} (s^{-1})	k_{obs2} (s^{-1})
WT	10.8	4.82
Trp108Phe	21.4	5.36
Tyr415Phe	5.43	1.25
Trp417Phe	7.22	1.02
Trp427Phe	9.01	0.9
Tyr415Phe/Trp417Phe	8.1	1.63

[a]Obtained by fitting traces in **Figure 4B** to Equation 1
[b]NicA2's FAD was reduced with one equivalent of dithionite (see Experimental Procedures)
[c]See **Scheme S2** for kinetic scheme and steps represented by rate constants.

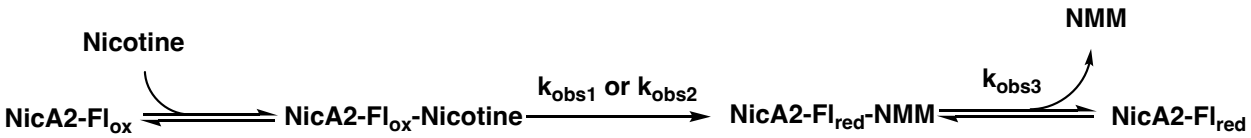

Scheme S1. Kinetic mechanism for NicA2's reductive half-reaction based on supplementary reference 5. NicA2-Fl_{ox}, NicA2 containing oxidized flavin; NicA2-Fl_{red}, NicA2 containing flavin hydroquinone; NMM, N-methylmyosmine.

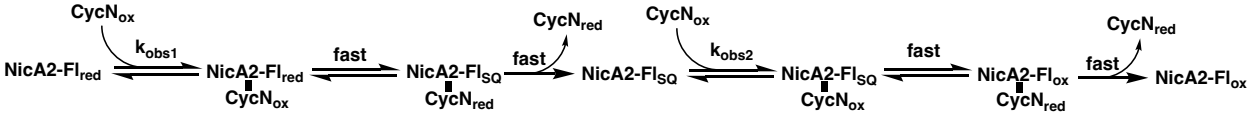

Scheme S2. Kinetic mechanism for NicA2's oxidative half-reaction based on supplementary reference 5. NicA2-Fl_{ox}, NicA2 containing oxidized flavin; NicA2-Fl_{SQ}, NicA2 containing flavin semiquinone; NicA2-Fl_{red}, NicA2 containing flavin hydroquinone; $CycN_{ox}$, CycN containing ferric heme; $CycN_{red}$, CycN containing ferrous heme.

Supplementary References:

(1) Evans, R., O'Neill, M., Pritzel, A., Antropova, N., Senior, A., Green, T., Žídek, A., Bates, R., Blackwell, S., Yim, J., Ronneberger, O., Bodenstein, S., Zielinski, M., Bridgland, A., Potapenko, A., Cowie, A., Tunyasuvunakool, K., Jain, R., Clancy, E., Kohli, P., Jumper, J., and Hassabis, D. (2022) Protein complex prediction with AlphaFold-Multimer. *bioRxiv* 2021.10.04.463034.

(2) Cianfrocco, M. A., Wong-Barnum, M., Youn, C., Wagner, R., and Leschziner, A. (2017) COSMIC2: A science gateway for cryo-electron microscopy structure determination. *ACM Int. Conf. Proceeding Ser. Part F1287*, 13–17.

(3) Tararina, M. A., Xue, S., Smith, L. C., Muellers, S. N., Miranda, P. O., Janda, K. D., and Allen, K. N. (2018) Crystallography Coupled with Kinetic Analysis Provides Mechanistic Underpinnings of a Nicotine-Degrading Enzyme. *Biochemistry 57*, 3741–3751.

(4) Choudhary, V., Wu, K., Zhang, Z., Dulchavsky, M., Barkman, T., Bardwell, J. C. A., and Stull, F. (2022) The enzyme pseudooxynicotine amine oxidase from Pseudomonas putida S16 is not an oxidase, but a dehydrogenase. *J. Biol. Chem. 298*, 102251.

(5) Dulchavsky, M., Clark, C. T., Bardwell, J. C. A., and Stull, F. (2021) A cytochrome c is the natural electron acceptor for nicotine oxidoreductase. *Nat. Chem. Biol. 17*, 344–350.

(6) Young, T. S., Ahmad, I., Yin, J. A., and Schultz, P. G. (2010) An Enhanced System for Unnatural Amino Acid Mutagenesis in E. coli. *J. Mol. Biol. 395*, 361–374.

(7) Majmudar, C. Y., Lee, L. W., Lancia, J. K., Nwokoye, A., Wang, Q., Wands, A. M., Wang, L., and Mapp, A. K. (2009) Impact of Nonnatural Amino Acid Mutagenesis on the in Vivo Function and Binding Modes of a Transcriptional Activator. *J. Am. Chem. Soc. 131*, 14240–14242.

(8) Feissner, R., Xiang, Y., and Kranz, R. G. (2003) Chemiluminescent-based methods to detect

subpicomole levels of c-type cytochromes. *Anal. Biochem. 315*, 90–94.

(9) Zabinski-Snopko, R. M., and Czerlinski, G. H. (1981) Spectrophotometric titrations of ferricytochrome C with ferrohexacyanide in the pH range 5 to 7. *J. Biol. Phys. 9*, 155–167.

(10) Moran, G. R. (2019) Anaerobic methods for the transient-state study of flavoproteins: The use of specialized glassware to define the concentration of dioxygen, in *Methods in Enzymology* 1st ed., pp 27–49. Elsevier Inc.

(11) Jurrus, E., Engel, D., Star, K., Monson, K., Brandi, J., Felberg, L. E., Brookes, D. H., Wilson, L., Chen, J., Liles, K., Chun, M., Li, P., Gohara, D. W., Dolinsky, T., Konecny, R., Koes, D. R., Nielsen, J. E., Head-Gordon, T., Geng, W., Krasny, R., Wei, G. W., Holst, M. J., McCammon, J. A., and Baker, N. A. (2018) Improvements to the APBS biomolecular solvation software suite. *Protein Sci. 27*, 112–128.

(12) Qiu, J., Wei, Y., Ma, Y., Wen, R., Wen, Y., and Liu, W. (2014) A novel (S)-6-hydroxynicotine oxidase gene from Shinella sp. Strain HZN7. *Appl. Environ. Microbiol. 80*, 5552–5560.

(13) Deay, D. O., Seibold, S., Battaile, K. P., Lovell, S., Richter, M. L., and Petillo, P. A. (2022) Improving the kinetic parameters of nicotine oxidizing enzymes by homologous structure comparison and rational design. *Arch. Biochem. Biophys. 718*, 109122.

(14) Fitzpatrick, P. F., Chadegani, F., Zhang, S., Roberts, K. M., and Hinck, C. S. (2016) Mechanism of the Flavoprotein L-Hydroxynicotine Oxidase: Kinetic Mechanism, Substrate Specificity, Reaction Product, and Roles of Active-Site Residues. *Biochemistry 55*, 697–703.

(15) Fitzpatrick, P. F., Chadegani, F., Zhang, S., and Dougherty, V. (2017) Mechanism of Flavoprotein L-6-Hydroxynicotine Oxidase: pH and Solvent Isotope Effects and Identification of Key Active Site Residues. *Biochemistry 56*, 869–875.

(16) Sablin, S. O., Yankovskaya, V., Bernard, S., Cronin, C. N., and Singer, T. P. (1998) Isolation and characterization of an evolutionary precursor of human monoamine oxidases A and B. *Eur. J. Biochem. 253*, 270–279.

(17) Atkin, K. E., Reiss, R., Koehler, V., Bailey, K. R., Hart, S., Turkenburg, J. P., Turner, N. J., Brzozowski, A. M., and Grogan, G. (2008) The Structure of Monoamine Oxidase from Aspergillus niger Provides a Molecular Context for Improvements in Activity Obtained by Directed Evolution. *J. Mol. Biol. 384*, 1218–1231.

(18) Tan, A. K., and Ramsay, R. R. (1993) Substrate-specific enhancement of the oxidative half-reaction of monoamine oxidase. *Biochemistry 32*, 2137–2143.

(19) Dunn, R. V., Marshall, K. R., Munro, A. W., and Scrutton, N. S. (2008) The pH dependence of kinetic isotope effects in monoamine oxidase A indicates stabilization of the neutral amine in the enzyme-substrate complex. *FEBS J. 275*, 3850–3858.